

RESEARCH REPORT

Comparative proteomic analysis reveals that juvenile hormone binding protein and adenylate kinase may be involved in the molting process of silkworm, *Bombyx mori*

Y Yang, L Chen, Q Tang, Y Zhang, H Tang, P Lü, Q Yao, K Chen

*Institute of Life Sciences, Jiangsu University, Zhenjiang 212013, China**Accepted October 13, 2017***Abstract**

The molting is an essential part of the silkworm metamorphosis development. Although previous studies have demonstrated that molting in silkworm is associated with prothoracicotropic hormone (PTTH), molting hormone (MH), and juvenile hormone (JH), the changes of proteins and genes during silkworm molting, as well as the molecular mechanism about its generating and maintaining remains unclear. In this paper, the proteomic approaches were employed to investigate this issue. Totally, 35 different proteins were successfully identified through mass spectrometry and database searches, among which 42 % proteins were involved in cell structure and 16 % proteins belonged to the metabolism group. Meanwhile, vacuolar ATP synthase, juvenile hormone binding protein precursor and adenylate kinase isoenzyme were found to be down-regulated at early, mid-molt stages, which were further confirmed by quantitative real-time polymerase chain reaction (qRT-PCR). Taken together, our data suggests that juvenile hormone binding protein (JHBP) and adenylate kinase (AK) play a critical role in the process of silkworm molting, which may participate in the regulation of silkworm molting.

Key Words: *Bombyx mori*; molting; proteomics; juvenile hormone binding protein; adenylate kinase

Introduction

Insects are the most abundant organisms in the world and encompass nearly 80 % species of our planet, which provide a large amount of desirable material for us to investigate the molecular basis of physiological mechanisms (Dahanukar *et al.*, 2005; Li *et al.*, 2010). The silkworm (*Bombyx mori*) has been fed as an important economic insect in sericulture industry. With the implementation and completion of whole genome sequencing program, silkworm has become a model insect of Lepidoptera molecular biological research (Xia *et al.*, 2004, 2009).

Molting is a common phenomenon in the developmental process of many organisms and is essential for the molecular, physiological and morphological rebuilding of living animals. In insect, molting is the regular shedding of the exoskeleton at specific points in its life cycle to let it grow. The previous studies have demonstrated that molting in silkworm is associated with their growth and other physiological processes and is a cascade process of gene expression and interaction (Kinjoh *et al.*, 2007; Muramatsu *et al.*, 2008; Wang *et al.*, 2013), which is endogenously controlled, involving in prothoracicotropic hormone (PTTH), molting hormone (MH), and juvenile hormone (JH). These hormones are secreted by the endocrine system, including brain neurosecretory cells, corpora allata and prothoracic glands, among which brain neurosecretory cells are dominant and play a central role. Although molting has been reasonably defined, the molecular regulation mechanism involved in generating and maintaining remains unclear. Meanwhile, the changes of genes or proteins during silkworm molting have not yet been resolved and it is also uncertain about which genes and proteins are indeed involved in the regulation of silkworm molting. These issues are very important for understanding the molecular mechanism of silkworm molting. Therefore, systematic studies are required to investigate these issues.

Corresponding author:

Keping Chen
Institute of Life Sciences Jiangsu University
301 Xuefu Road, Zhenjiang
Jiangsu Province 212013, PR China
E-mail: kpchen@ujs.edu.cn

List of abbreviations:

ACN, acetonitrile; CBB, Coomassie Brilliant Blue; IEF, isoelectric focusing; MALDI-TOF MS, matrix-assisted laser desorption/ionization time of flight mass spectrometry; PMSF, phenylmethanesulfonyl fluoride; SDS-PAGE, sodium dodecyl sulphate polyacrylamide gel electrophoresis; TFA, trifluoroacetic acid; 2-DE, two-dimensional electrophoresis

In recent years, the proteomic approaches, including two-dimensional electrophoresis and mass spectrometry, have been applied successfully to identify the specific proteins from different tissues and organs of silkworm, such as haemolymph (Li *et al.*, 2006; Hou *et al.*, 2010; Liu *et al.*, 2010), fat body (Moghaddam *et al.*, 2008), midgut (Qin *et al.*, 2012; Feng *et al.*, 2014; Kannan *et al.*, 2016), silk gland (Zhang *et al.*, 2006; Jia *et al.*, 2007; Yi *et al.*, 2013), endocrine organs, larval head (Li *et al.*, 2010; Li *et al.*, 2016; Arunprasanna *et al.*, 2017), and so on. These results from proteome provided important evidences and clues for understanding the growth and development of silkworm. The silkworm is metamorphic molts involving in complex hormonal regulation and replacement of cuticle types and can be considered a model organism for understanding molting and metamorphosis in holometabolous insects. The insect head is composed of important sensory systems, including the olfactory, visual, gustatory organs, and some important endocrine organs, which can receive environmental stimuli and regulate insect growth and development. Therefore, insect head plays a crucial role in insect growth, reproduction, diapause, and metamorphosis processes (Li *et al.*, 2009; Li *et al.*, 2010; Li *et al.*, 2016; Wang *et al.*, 2016). In current study, the proteomic approach was employed to detect and identify differentially expressed proteins from silkworm larval heads, which allowed us to determine the proteins and genes associated with molting and decipher the molecular mechanism of silkworm molting.

Materials and Methods

Experimental insects and developmental stage

The hybrid strain Jingsong×Haoyue of the silkworm *B. mori* were used for this experiment, which was provided by Sericultural Research of Institute, Chinese Academy of Agricultural Sciences, Zhenjiang, China. All larvae were reared with the fresh mulberry leaves at 25 ± 1 °C and 75 ± 2 % relative humidity (photoperiod 16 h light: 8 h dark). The larvae of 1st - 3rd instar were fed with the chopped tender leaves and 4th - 5th instar larvae were fed with the matured leaves. The silkworm larval heads were used for proteomic analysis, which were collected at specific time points during the molt from the penultimate (4th) to the last (5th) larval instar. Based on the time of head capsule slippage (HCS) occurring at the fourth molt period, the molting stage was determined, that is, HCS occurring (denoted by mq), 12 h and 24 h after HCS (denoted by m1 and m2), and newly molted fifth instar larvae (denoted by qc). The larval heads were collected on ice, immediately frozen in liquid nitrogen and stored at -70 °C for later use (at least 100 heads of each sample). The experiments were repeated three times.

Protein sample preparation

The larval heads of silkworm were grounded into fine powder in liquid nitrogen and homogenized on ice for 5 min in pre-cooled extraction buffer (20 mM Tris-HCl pH 7.5, 250 mM sucrose, 10 mM EGTA, 1 mM PMSF, 1 mM DTT, and 1 % Triton (v/v) X-100)

as described by Cilia *et al.* (Cilia *et al.*, 2009). The homogenate was transferred into the 2.0 mL centrifuge tube and centrifuged (12,000g, 4 °C, 30 min). The supernatant was collected and equal-volume tris-saturated phenol was added and mixed. The phenol layer containing proteins was collected and incubated 10 ~ 12 h at -20 °C with methanol solution containing 100 mM ammonium acetate. After centrifugation (12,000g, 30 min, 4 °C), the supernate was discarded. The precipitate was washed again with methanol solution containing 100 mM ammonium acetate and then washed 4 ~ 5 times using ice-cold acetone containing 13 mM DTT, centrifuged (12,000g, 4 °C, 20 min/each time), and vacuum-dried. The dried powder was dissolved in lysis buffer (7 M urea, 2 M thiourea, 4 % w/v CHAPS, 2 % v/v Bio-lyte, pH 3 - 10, 1 % w/v DTT), overnight at 4 °C. Finally, the mixtures were centrifuged (12,000g, 20 min, 4 °C). The supernatant was collected and used for two-dimensional electrophoresis. The protein concentration was measured by Bradford method (Bradford, 1976).

Two-dimensional electrophoresis (2-DE)

IEF was carried out through Bio-Rad PROTEAN electrophoresis system and 17 cm immobilized IPG dry gel strips with pH 4 - 7 liner range (Bio-Rad, USA) was used. About 1.5 mg protein samples were loaded by passive rehydration (room temperature, 11 ~ 12 h). Then IEF was performed at 300, 500, and 1,000 V, linear for 1 h, respectively, next 10,000 V, linear for 5 h, and then remained 10,000 V until a total voltage of 54,000 Vh. Subsequently, the gel strips were equilibrated for 15 min in equilibration buffer (0.05 M Tris-HCl pH 6.8, 2.5 % w/v SDS, 30 % v/v glycerol and 1 % w/v DTT) and then equilibrated for 15 min again (0.05 M Tris-HCl pH 6.8, 2.5 % w/v SDS, 30 % v/v glycerol and 2.5 % w/v iodoacetamide). The second dimension SDS-PAGE was carried out with a Laemmli buffer system (15% resolving gels) (Laemmli, 1970). Finally, the gels were dyed with 0.116 % CBB R-250 (0.116 % w/v CBB, 25 % v/v ethanol, and 8 % v/v acetic acid).

Image and data analysis

The 2-DE gels were scanned using the imagescanner III (GE Healthcare Life Sciences). The images were analyzed using ImageMaster 7.0 software (GE Healthcare Life Sciences). The optimized parameters were as follows: saliency = 3, smooth = 6, and minimum area = 60. The value of each protein spot was normalized (a percentage of the total volume in the whole set of gel spots). The protein spots with ratios ≥ 1.5 or ratios ≤ 0.67 and passing the Student's *t*-test ($p < 0.05$) were considered to be differentially expressed proteins.

In-gel digestion and protein identification

The differentially expressed proteins were manually cut down from the gels and washed using ultrapure water. The gel pieces were destained 2 ~ 3 times by ultrasonic with 50 μ L destaining buffer (50 % ACN, 25 mM NH_4HCO_3) until the gel pieces became colorless. Next, the gel pieces were rinsed using 25 mM NH_4HCO_3 , 50 % ACN, and 100 % CAN (50 μ L/each), respectively, and vacuum-dried. The

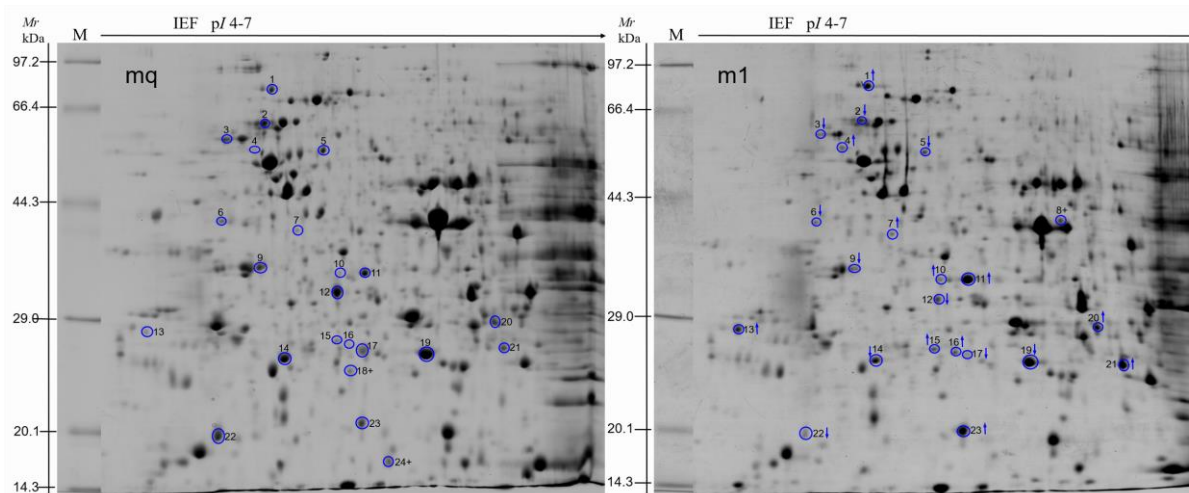


Fig. 1 The 2-DE profiles from head extracted proteins between mq and m1. Note: (Reference gel: mq). The differentially expressed protein spots are indicated by circles and labeled with Arabic numerals. The upward and downward arrows respectively indicate up-regulated and down-regulated proteins. The protein spots with circles and plus symbol indicate that the protein spot is expressed only in this 2-DE gel. The numbers shown on the left indicate the protein markers in kDa. (Figs 2 and 3 are same as Fig. 1)

dried gel pieces were soaked in 25 mM NH_4HCO_3 with 10 $\mu\text{g}/\text{mL}$ of trypsin (Promega, USA) at 4 °C for 30 min. Subsequently, 10 ~ 15 μL 25 mM NH_4HCO_3 was added to the gel pieces and the gel pieces were digested at 37 °C overnight (about 12 h). Peptides were collected and dried by vacuum (-50 °C) and then stored at -70 °C until mass spectrometry. MALDI TOF/TOF samples were prepared by spotting 2 μL digested protein solution (dissolved with 5 μL 0.1 %TFA) and 1 μL matrix (α -cyano-4-hydroxycinnamic acid, Sigma, 10 mg/mL, dissolved in 50 % ACN containing 0.1 % TFA) on the 600 μm AnchorChip MALDI probe (Bruker Daltonik, Germany). After dryness at room temperature, the samples were analyzed through MALDI TOF/TOF Mass Spectrometer (Bruker Daltonik, Germany). All the acquired peptide mass finger prints of MALDI-TOF MS/MS data were analyzed through the BioTools 3.0 program to search the protein database (NCBI nr) using in-house Mascot software (Matrix Science, UK). Metazoa (Animals) was selected as the taxonomic category. To ensure the confidence of identified results, the search parameters were set as follows: trypsin was selected as enzyme, one missed cleavage was allowed, carbamidomethyl was selected as fixed modification, Gln->pyro-Glu (N-term Q) was chosen as variable modification, and peptide tolerance was set at ± 100 ppm with a MH^+ mass values. The proteins whose Mascot scores were more than 55 were considered to be reliably identified.

Gene ontology (GO) analysis

To evaluate the major biological functions of the differentially expressed proteins among mq-m1, mq-m2, and mq-qc, Gene Ontology (GO) analysis (<http://www.geneontology.org/>) was employed. The GO IDs of all identified proteins were obtained by InterProScan searching

(<http://www.ebi.ac.uk/interpro/scan.html>) using the amino acid sequences. Following the Ye's method (Ye *et al.*, 2006), the annotation information of identified proteins was gathered and then uploaded as Web Gene Ontology Annotation Plot (WEGO) Native Format into WEGO (<http://wego.genomics.org.cn/cgi-bin/wego/index.pl>). Finally, the GO plot was obtained and downloaded as jpeg format. According to WEGO, all identified proteins was classified as molecular function, cellular component and biological process (Ye *et al.*, 2006).

RNA extraction and quantitative real-time PCR (qRT-PCR)

Using Trizol reagent (Invitrogen, USA), total RNA was extracted and 1 μg RNA was used for the first strand synthesis. The specific primers were shown in Table S1. The qRT-PCR was performed in a total volume of 20 μL containing 2 μL of cDNA (200 ng), 10 μL of SYBR Green Master Mix (Vazyme Biotech Co., Ltd, China), 0.4 μL of 50 \times ROX Reference Dye I, 0.4 μL of primers (10 μM) and 7.2 μL of H_2O . Amplification was carried out using an ABI7300 PCR thermocycler (Applied Biosystems, USA) as follows: 5 min at 95 °C, followed by 40 cycles of 10 s at 95 °C, 31 s at 60 °C and one cycle of 15 s at 95 °C, 60 s at 60 °C, 15 s at 95 °C. The α -tubulin gene (NCBI accession No. NM_001043419.1) of silkworm was amplified as a reference and the experiments were repeated three times.

Results

Differentially expressed proteins between mq-m1, mq-m2, and mq-qc

To investigate the molecular mechanism of silkworm molting, we applied proteomic approach to

comprehensively identify and then characterize the differentially expressed proteins during the fourth molt of silkworm. As shown in Figures 1, 2 and 3, most protein spots were mainly distributed in the range of pH 4 - 7 and mass weight 20 - 100 kDa, indicating that protein samples were correctly extracted and most proteins from the larval heads of silkworm were obtained. Totally, 842 ± 15 , 825 ± 13 , 827 ± 10 , 857 ± 16 protein spots were detected in

mq, m1, m2, and qc, respectively, in CBB R-250 stained gels. Using ImageMaster 7.0 software, 24, 20, and 18 different protein spots were ultimately determined between mq-m1, mq-m2, and mq-qc, respectively (Supplementary file, Table S2). Through further analysis, these 62 differentially expressed proteins can be classified into 35 different proteins, which were numbered uniformly (Table 1) and labeled in Figures 1, 2 and 3.

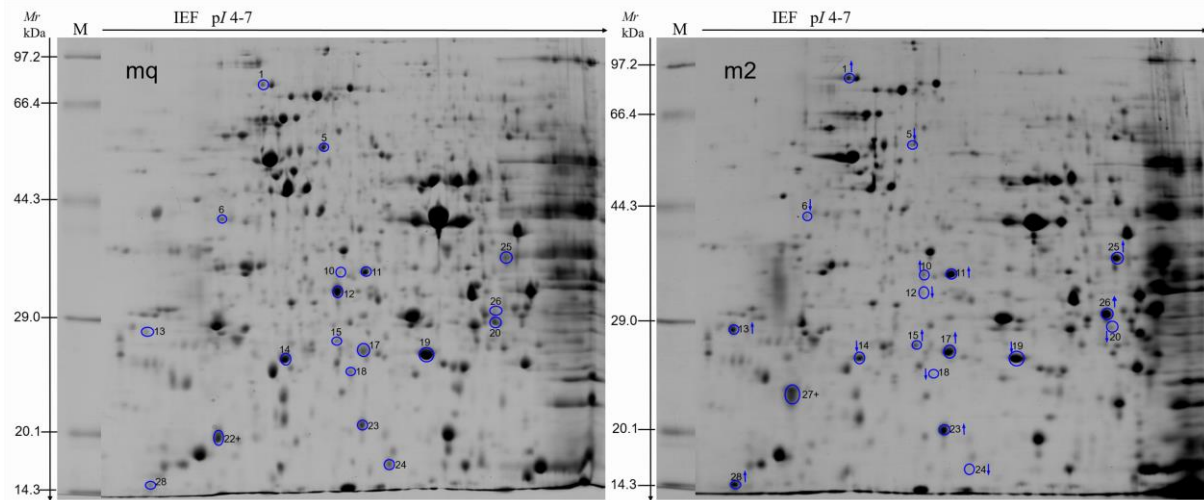


Fig. 2 The 2-DE profiles from head extracted proteins between mq and m2.

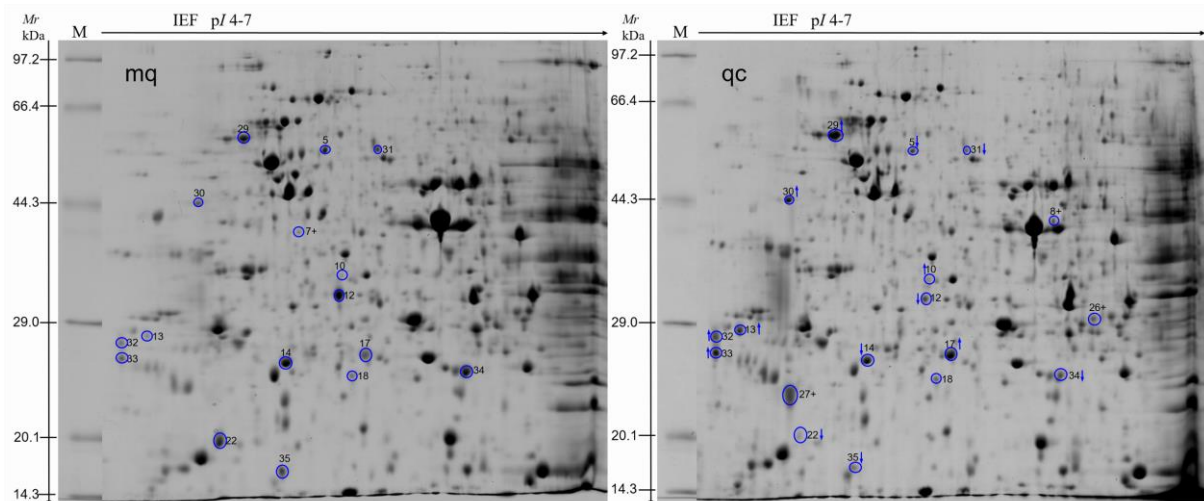


Fig. 3 The 2-DE profiles from head extracted proteins between mq and qc.

MALDI-TOF MS/MS identification of differentially expressed proteins and functional classification

Among 35 differentially expressed proteins, 34 proteins were successfully identified through MALDI-TOF MS/MS and database searches (Mascot score > 55), and one protein was identified through MALDI-TOF MS and database searches (Mascot score > 84) (Table 1). According to Bevan

et al. (1998), these 35 proteins can be divided into the following nine categories: cell structure proteins, metabolism-related proteins, disease/defense-related proteins, transporter, transcription, molecular chaperone, secondary metabolism, protein synthesis, and unknown function proteins (Fig. 4). As shown in Figure 4, 42 % of the identified proteins were classified into the

Table 1 Identification of differentially expressed proteins by MALDI-TOF MS/MS

Spot No.	Protein name	Accession No.	Mr(kDa)/pI ^a	Mascot scores	SC ^b (%)	Amino acid	Function
1	heat shock protein 70-3	AEI58998	72.82/5.12	138	25%	655	Molecular chaperone
2	tubulin alpha-3 chain, partial	KFQ41598	43.57/5.79	197	55%	389	Cell structure
3	beta-1 tubulin	TBB1_MANSE	50.65/4.75	262	64%	447	Cell structure
4	uncharacterized protein LOC101738727	XP_012552185	49.91/5.29	129	31%	449	Unknown function
5	vacuolar ATP synthase subunit b	NP_001091828	54.67/5.25	187	55%	490	Metabolism
6	antichymotrypsin-2	ACH2_BOMMO	41.43/5.26	109	39%	375	Metabolism
7	antitrypsin isoform 1	ACT36276	43.46/5.41	145	41%	392	Metabolism
8	uncharacterized LOC101739385	XP_004922152	37.46/6.07	91	32%	328	Unknown function
9	annexin	BAB16697	36.11/4.89	138	43%	323	Disease and defense
10	alpha-tocopherol transfer protein-like	XP_004928929	35.28/5.56	146	47%	306	Transporter
11	alpha-tocopherol transfer protein-like	XP_004928929	35.28/5.56	183	50%	306	Transporter
12	juvenile hormone binding protein brP-2095 precursor	NP_001036987	28.05/5.42	140	55%	249	Secondary metabolism
13	cuticular protein RR-1 motif 34 precursor	NP_001166717	23.18/4.78	107	56%	207	Cell structure
14	adenylate kinase isoenzyme 1	XP_004929167	25.29/5.70	108	57%	226	Metabolism
15	tumor protein D54 isoform X3	XP_004930117	22.32/5.41	91	28%	206	Cell structure
16	putative cuticle protein	FAA00454	21.66/5.39	91	45%	215	Cell structure
17	H ⁺ transporting ATP synthase subunit d	NP_001093279	20.19/5.56	57	52%	179	Metabolism
18	transcription factor BTF3 homolog 4	XP_012551703	19.04/9.12	201	48%	174	Transcription
19	triosephosphate isomerase	NP_001119730	26.93/5.67	168	64%	248	Metabolism
20	odorant binding protein fmxg18C17 precursor	NP_001157372	26.48/6.23	121	28%	236	Cell structure
21	glutathione S-transferase sigma 1	NP_001037077	23.60/5.98	131	54%	206	Disease and defense
22	cuticular protein RR-1 motif 42 precursor	NP_001166712	17.17/5.16	151	86%	159	Cell structure
23	actin-depolymerizing factor 1	NP_001093278	17.23/6.17	175	64%	148	Cell structure
24	muscular protein 20	NP_001040476	20.29/8.70	79	20%	184	Cell structure
25	cuticular protein 66D	NP_729400	30.80/5.97	74	20%	270	Cell structure
26	cuticular protein RR-2 motif 67 precursor	NP_001166691	18.72/6.16	223	43%	178	Cell structure
27	uncharacterized protein LOC101741978	XP_004930780	16.55/4.93	117	46%	144	Unknown function
28	ribosomal protein P2	NP_001037213	11.53/4.68	121	16%	112	Protein synthesis
29	beta tubulin	NP_001036887	50.72/4.83	267	70%	447	Cell structure
30	centromere protein F isoform X2	XP_004926842	33.22/4.84	157	30%	297	Cell structure
31	T-complex protein 1 subunit epsilon-like	XP_004933262	59.19/5.63	127	31%	542	Molecular chaperone
32	cuticular protein RR-1 motif 3 precursor	NP_001166744	14.68/4.66	93	28%	137	Cell structure
33	cuticular protein RR-1 motif 3 precursor	NP_001166744	14.68/4.66	64	26%	137	Cell structure
34	thiol peroxidoredoxin	NP_001037083	22.07/6.09	252	18%	195	Disease and defense
35	ubiquitin-like protein SMT3	NP_001037410	10.36/5.29	105	23%	91	Transcription

^a MW: Molecular weight; pI: Isoelectric point^b SC: Sequence coverage^c The identified protein by MALDI-TOF MS

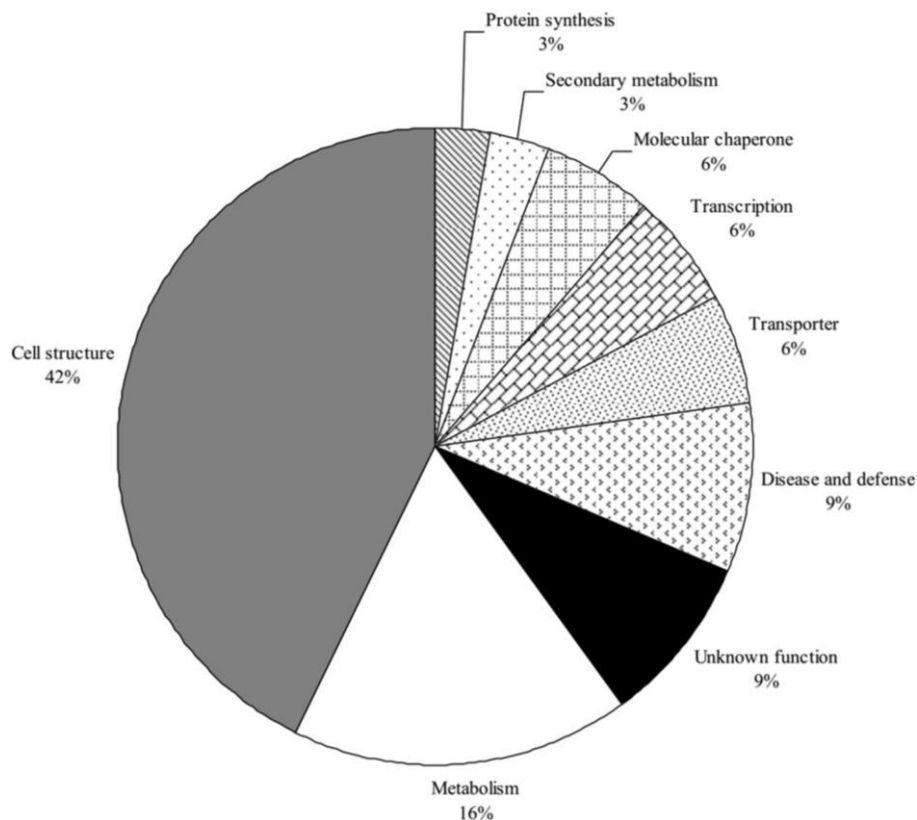


Fig. 4 Functional classifications of the identified proteins.

cell structure group, 16 % proteins belonged to the metabolism group, which accounted for 58 % of the identified proteins and were the most abundant proteins in the heads of silkworm larvae. Compared with HCS occurring stage, up-regulated proteins in early, mid-molt of the fourth molt period, and newly molted fifth instar larvae mainly involved in cell structure, but down-regulated proteins mainly involved in metabolism (Supplementary file, Table S1). In particular, four metabolism/secondary metabolism-related proteins were found to express regularly (Fig. 5, spot nos. 5, 12, 14, 17). Among these four proteins, spot no. 5, 12 and 14 highly expressed at HCS occurring stage, and then gradually declined at early, mid-molt stages, especially spot no. 5 and 12. At newly molted fifth instar larvae stage, the expression levels of these proteins increased again (Fig. 5). As shown in Table 1, these proteins were vacuolar ATPase subunit b, juvenile hormone binding protein brP-2095 precursor, adenylate kinase isoenzyme 1, H⁺ transporting ATP synthase subunit d, respectively. Meanwhile, we also identified some stress and/or defense-related proteins, including annexin (Table 1, Fig. 1, spot no. 9), glutathione S-transferase sigma 1 (Table 1, Fig. 1, spot no. 21), thiol peroxidoredoxin (Table 1, Fig. 3, spot no. 34). As shown in Table 1 and Figure 1, annexin was down-regulated at 12 h after HCS (m1), whereas glutathione S-transferase was up-regulated at 12 h after HCS (m1). The expression level of thiol peroxidoredoxin had no obvious change among HCS

(mq), 12 h after HCS (m1), and 24 h after HCS (m2), but its expression level was significantly down-regulated at newly molted fifth instar larvae (qc) stage (Table 1, Fig. 3, spot no. 34).

GO analysis

All GO annotations of differentially expressed proteins were summarized and used for GO analysis. As shown in Figure 6, these proteins mainly involved in cell, cell part, organelle, organelle part, binding, catalytic, structural molecule, cellular process, and metabolic process, which were consistent with its specific developmental stages. The GO analysis can provide useful clues for subsequent studies of physiological roles and characteristics of these identified proteins.

Quantitative real-time PCR

In current study, four proteins (spot no. 5, vacuolar ATP synthase subunit b; spot no. 12, juvenile hormone binding protein brP-2095 precursor; spot no. 14, adenylate kinase isoenzyme 1; spot no. 17, H⁺ transporting ATP synthase subunit d) were selected to investigate their expression patterns at transcript level. As shown in Figure 7, vacuolar ATP synthase subunit b (spot no. 5) and H⁺ transporting ATP synthase subunit d (spot no. 17) displayed good correlation between transcript and protein levels at each time point. Compared with 12 h and 24 h after HCS (m1 and m2), juvenile hormone binding protein brP-2095 precursor (spot no. 12) and

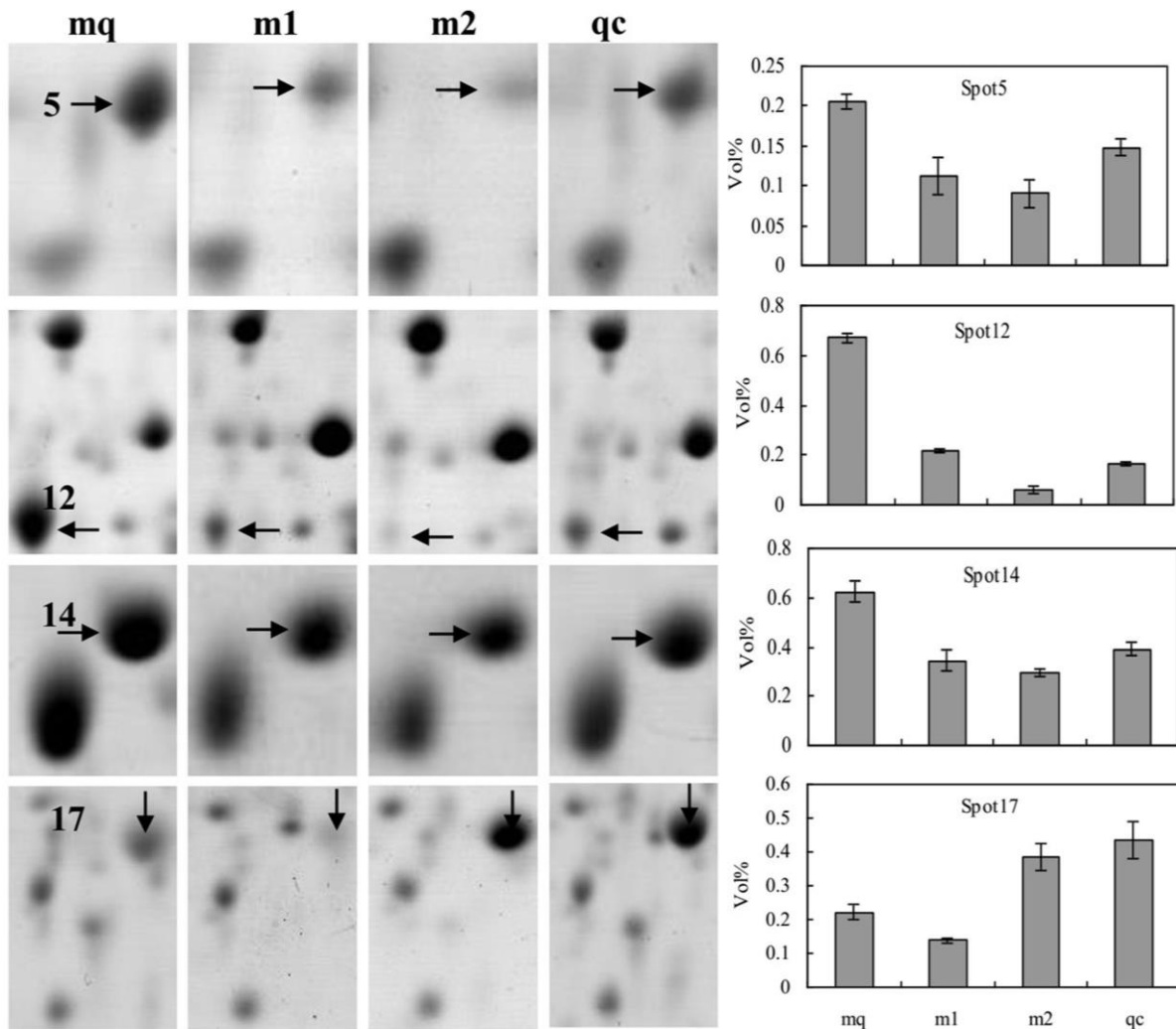


Fig. 5 Enlarged view of distribution of regularly changed proteins. Changed proteins were indicated by black arrows, spot numbers were shown on the first column, and the quantitative changes of proteins were shown in the last column (Vol %: spot relative volume). Values are average of three replicates.

adenylate kinase isoenzyme (spot no. 14) were both up-regulated at transcript and protein levels at mq and qc stages (Fig. 7). The quantitative real-time PCR results demonstrated that the expression patterns of these proteins at transcript level were basically consistent with the proteomic results.

Discussion

In this study, we applied proteomic approach to globally identify different proteins during the fourth molting of silkworm and evaluate proteomic dynamic changes and their roles in this specific period. Taken together, 35 differentially expressed proteins were successfully identified through mass spectrometry and database searches. Among these identified proteins, 42 % proteins were classified as the cell structure group, which were the most abundant proteins in silkworm larval heads of the fourth molting stage, indicating that cell components of the heads at this stage changed dramatically. Moreover,

down-regulated proteins at early, mid-molt, and newly molted fifth instar larvae mainly consisted of metabolism-related proteins, indicating the metabolic levels at these stages were very low, which were consistent with its specific developmental period. Interestingly, the expression levels of three metabolism/secondary metabolism-related proteins were down-regulated significantly at early, mid-molt stages (Fig. 5, spot nos. 5, 12, 14), which were further confirmed by quantitative real-time PCR. Meanwhile, these three proteins had the Mascot scores with 187, 140, and 108, and their sequence coverages were 55 %, 52 %, and 57 %, which strongly supported for their positive identification (Table 1, Supplementary files, Figs S1, S2, S3). The vacuolar ATPase (V-ATPase) is a heteromultimeric protein complexes that consists of the peripheral V1 domain and the integral V0 domain, which is ATP-driven proton pumps and can transport protons across the plasma membrane (Beyenbach and Wiczorek, 2006; Forgac, 2007;

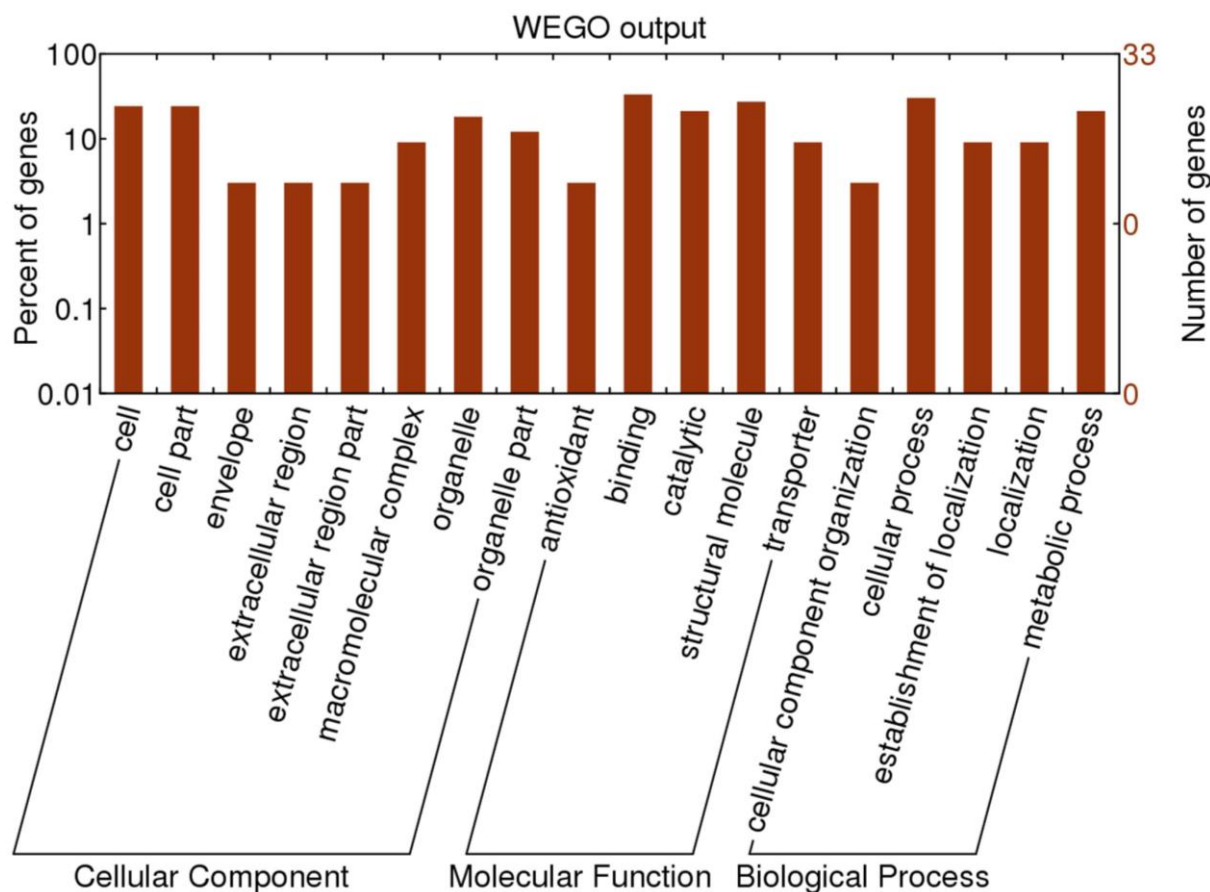


Fig. 6 The Gene Ontology (GO) analysis (Web Gene Ontology Annotation Plot) for differentially expressed proteins. The left coordinate axis represents the proportion of proteins for every GO annotation, and the right one indicates the number of proteins for each GO annotation.

Collaco *et al.*, 2013; Lv *et al.*, 2014). V-ATPases are essential for pH regulation of the intracellular compartments, the extracellular space, and the cytoplasm and play a vital role in acidification of organelles within the lysosomal, endocytic, and secretory pathways (Breton and Brown, 2007; Collaco *et al.*, 2013). The juvenile hormone binding proteins (JHBPs) are specific carriers of juvenile hormone (JH) and also the first member in the series of proteins participating in JH signal transmission (Sok *et al.*, 2005). As the key proteins in JH signaling, JHBPs can not only transport JH to its target tissues where JH exerts a physiological effect (Goodman, 1990), but also inhibit enzymatic degradation of JH through general hemolymph esterases (Ritdachyeng *et al.*, 2012). Previous studies have pointed out that more than 99.8 % JH in hemolymph emerges in a complex with JHBPs and the interaction between JH and its carrier partner protein is specific (Ozyhar and Kochman, 1987; Touhara *et al.*, 1993; Ritdachyeng *et al.*, 2012). It is well known that JH plays pivotal roles in regulating insect growth and development, especially in maintaining the larval state, which ensures growth of the larva and prevents metamorphosis (Riddiford, 1994; Vermunt *et al.*, 2001). Therefore, as JH signal transmitters and

specific carrier proteins, information concerning JHBPs not only provides an alternative approach to understand how JH regulates metamorphosis, but also affords important clues for us to investigate the molecular mechanism of silkworm molting. Previous studies have shown that JH regulates metamorphosis by way of specific gene up-regulation and down-regulation (Riddiford, 1994; Truman and Riddiford, 1999; Gilbert *et al.*, 2000). In current study, although JH was not detected, the precursor of its carrier protein decreased significantly during silkworm molting. These observations suggest that JH regulates metamorphosis by way of JHBP down-regulation, that is, JHBP indirectly participates in the regulation of silkworm molting and plays a crucial role during silkworm molting (Fig. 8, A pathway). Adenylate kinase (AK) is ubiquitous in a variety of organisms and can catalyze a reversible high energy phosphoryl transfer reaction between ATP and AMP to generate ADP (Noda, 1973; Miura *et al.*, 2001), which facilitates to regulate AMP levels. The previous study has demonstrated that the blood AMP levels are potential metabolic signals related to vital functions, including body energy sensing, sleep, hibernation and food intake (Dzeja and Terzic, 2009).

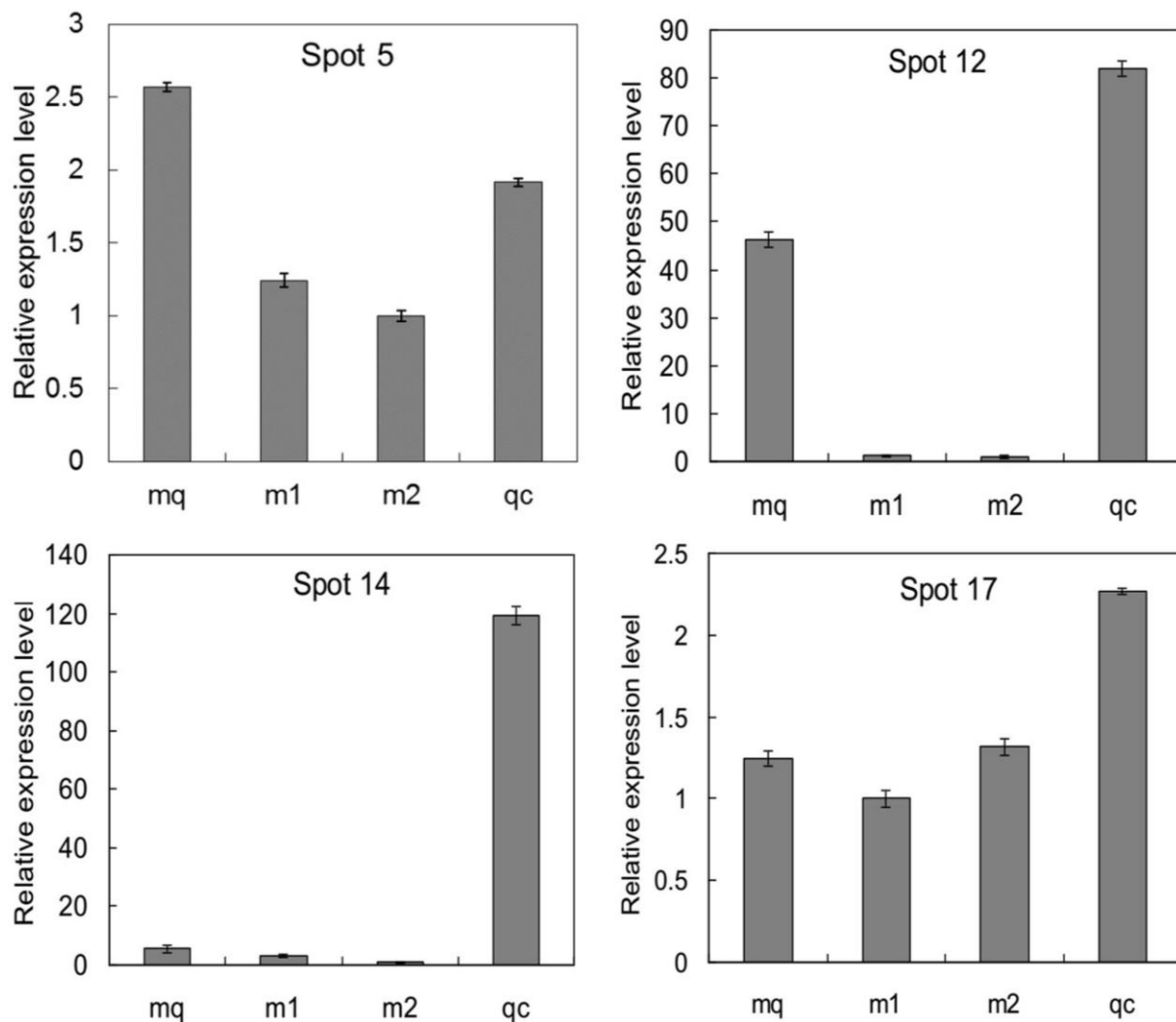


Fig. 7 Relative expression levels of spot nos. 5, 12, 14 and 17. X-axis represents different samples, Y-axis represents the relative expression level of each protein.

The energy from adenylate kinase-catalyzed phosphotransfer can regulate multiple extracellular and intracellular energy-dependent and nucleotide signaling processes, including cell and ciliary motility, excitation-contraction coupling, energetics of cell cycle, DNA synthesis and repair, hormone secretion, nuclear transport, and developmental programming (Dzeja and Terzic, 2009). In current study, the expression levels of AK isoenzyme at HCS and newly molted fifth instar larvae stages were higher than that at early, mid-molt stages. As mentioned above, AMP levels were associated with some crucial functions, such as body energy sensing, sleep and hibernation. Therefore, we postulated that AK may function as a mediator that control developmental events such as diapause, molting and eclosion, which was firstly found that AK might be correlated with silkworm molting (Fig. 8, B pathway). These findings described here not only improve our understanding of the molecular mechanism of silkworm molting, but also

demonstrate that comparative proteomic approach can be conducive to identifying different proteins and investigating their roles in silkworm studies.

Conclusions

In current study, proteomic method was employed to investigate and analyze the changes of different proteins during silkworm molting, which enabled us to better understand the molecular mechanism of molting. Eventually, 35 different proteins were successfully identified, including juvenile hormone binding protein precursor and adenylate kinase isoenzyme. The identification of these two proteins suggests that JHBPs and AK may take part in the regulation of silkworm molting. As a consequence, our results not only provide novel insights and references for the explanation of molecular mechanism of silkworm molting, but also provide candidate proteins and genes for the following investigations of their roles in silkworm molting.

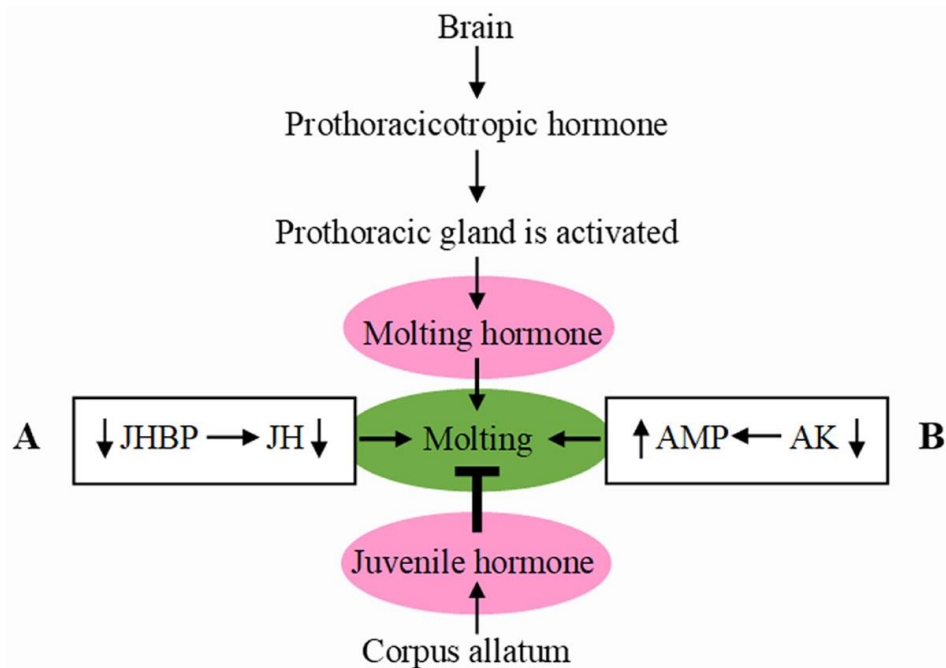


Fig. 8 The speculative molecular mechanism of silkworm molting.

Acknowledgments

This work was supported by National Natural Science Foundation of China (31572467), the Priority Academic Program Development of Jiangsu Higher Education Institutions, the Scientific Research Promotion Fund for the Talents of Jiangsu University (11JDG049). We are thankful to the anonymous reviewers for reviewing our manuscript and providing helpful comments and suggestions.

References

- Arunprasanna V, Kannan M, Anbalagan S, Krishnan M. Comparative proteomic analysis of larva and adult heads of silkworm, *Bombyx mori* (Lepidoptera: Bombycidae). *J. Entomol.* 1-12, 2017.
- Bevan M, Bancroft I, Bent E, Love K, Goodman H, Dean C, *et al.* Analysis of 1.9 Mb of contiguous sequence from chromosome 4 of *Arabidopsis thaliana*. *Nature* 391: 485-488, 1998.
- Beyenbach KW, Wieczorek H. The V-type H⁺ ATPase: molecular structure and function, physiological roles and regulation. *J. Exp. Biol.* 209: 577-589, 2006.
- Bradford MM. A rapid and sensitive method for the quantitation of microgram quantities of protein utilizing the principle of protein-dye binding. *Anal. Biochem.* 72: 248-254, 1976.
- Breton S, Brown D. New insights into the regulation of V-ATPase-dependent proton secretion. *Am. J. Physiol.-Renal.* 292: 10, 2007.
- Cilia M, Fish T, Yang X, McLaughlin M, Thannhauser TW, Gray S. A comparison of protein extraction methods suitable for gel-based proteomic studies of aphid proteins. *J. Biomol. Tech.* 20: 201-215, 2009.
- Collaco AM, Geibel P, Lee BS, Geibel JP, Ameen NA. Functional vacuolar ATPase (V-ATPase) proton pumps traffic to the enterocyte brush border membrane and require CFTR. *Am. J. Physiol - Cell Physiol.* 305: C981-C996, 2013.
- Dahanukar A, Hallem EA, Carlson JR. Insect chemoreception. *Curr. Opin. Neurobiol.* 15: 423-430, 2005.
- Dzeja P, Terzic A. Adenylate kinase and AMP signaling networks: metabolic monitoring, signal communication and body energy sensing. *Int. J. Mol. Sci.* 10: 1729-1772, 2009.
- Feng F, Chen L, Lian C, Xia H, Zhou Y, Yao Q, *et al.* Comparative proteomic analysis reveals the suppressive effects of dietary high glucose on the midgut growth of silkworm. *J. Proteomics* 108: 124-132, 2014.
- Forgac M. Vacuolar ATPases: rotary proton pumps in physiology and pathophysiology. *Nat. Rev. Mol. Cell Biol.* 8: 917-929, 2007.
- Gilbert LI, Granger NA, Roe RM. The juvenile hormones: historical facts and speculations on future research directions. *Insect Biochem. Mol.* 30: 617-644, 2000.
- Goodman WG. Biosynthesis, titer regulation and transport of juvenile hormones, in: Gupta, AP (ed.), *Morphogenetic Hormones of Arthropods. Discoveries, Syntheses, Metabolism, Evolution, Mode of Action and Techniques.* Rutgers University Press, New Brunswick, pp 83-124, 1990.
- Hou Y, Zou Y, Wang F, Gong J, Zhong X, Xia Q, *et al.* Comparative analysis of proteome maps of silkworm hemolymph during different developmental stages. *Proteome Sci.* 8: 2010.

- Jia SH, Li MW, Zhou B, Liu WB, Zhang Y, Miao XX, *et al.* Proteomic analysis of silk gland programmed cell death during metamorphosis of the silkworm *Bombyx mori*. *J. Proteome Res.* 6: 3003-3010, 2007.
- Kannan M, Suryaaathmanathan V, Saravanakumar M, Jaleel A, Romanelli D, Tettamanti G, *et al.* Proteomic analysis of the silkworm midgut during larval-pupal transition. *Inv. Surv. J.* 13: 191-204, 2016.
- Kinjoh T, Kaneko Y, Itoyama K, Mita K, Hiruma K, Shinoda T. Control of juvenile hormone biosynthesis in *Bombyx mori*. Cloning of the enzymes in the mevalonate pathway and assessment of their developmental expression in the corpora allata. *Insect Biochem. Mol.* 37: 808-818, 2007.
- Laemmli UK. Cleavage of structural proteins during the assembly of the head of bacteriophage T4. *Nature* 227: 680-685, 1970.
- Li JY, Chen X, Fan W, Moghaddam SHH, Chen M, Zhou ZH, *et al.* Shotgun strategy-based proteome profiling analysis on the head of silkworm *Bombyx mori*. *Amino Acids* 39: 751-761, 2009.
- Li JY, Chen X, Fan W, Moghaddam SH, Chen M, Zhou ZH, *et al.* Proteomic and bioinformatic analysis on endocrine organs of domesticated silkworm, *Bombyx mori* L. for a comprehensive understanding of their roles and relations. *J. Proteome Res.* 2620-2632, 2009.
- Li XH, Wu XF, Yue WF, Liu JM, Li GL, Miao YG. Proteomic analysis of the silkworm (*Bombyx mori* L.) hemolymph during developmental stage. *J. Proteome Res.* 5: 2809-2814, 2006.
- Li Y, Wang X, Chen Q, Hou Y, Xia Q, Zhao P. Metabolomics analysis of the larval head of the silkworm, *Bombyx mori*. *Int. J. Mol. Sci.* 17: 1460, 2016.
- Liu X, Yao Q, Wang Y, Chen K. Proteomic analysis of nucleopolyhedrovirus infection resistance in the silkworm, *Bombyx mori* Lepidoptera: Bombycidae. *J. Invertebr. Pathol.* 105: 84-90, 2010.
- Lv X, Huang L, Chen W, Wang X, Huang Y, Deng C, *et al.* Molecular characterization and serological reactivity of a vacuolar ATP synthase subunit ϵ -like protein from *Clonorchis sinensis*. *Parasitol. Res.* 113: 1545-1554, 2014.
- Miura K, Inouye S, Sakai K, Takaoka H, Kishi F, Tabuchi M, *et al.* Cloning and characterization of adenylate kinase from *Chlamydia pneumoniae*. *J. Biol. Chem.* 276: 13490-13498, 2001.
- Moghaddam SHH, Du X, Li J, Cao J, Zhong B, Chen Y. Proteome analysis on differentially expressed proteins of the fat body of two silkworm breeds, *Bombyx mori*, exposed to heat shock exposure. *Biotechnol. Bioproc. E.* 13: 624-631, 2008.
- Muramatsu D, Kinjoh T, Shinoda T, Hiruma K. The role of 20-hydroxyecdysone and juvenile hormone in pupal commitment of the epidermis of the silkworm, *Bombyx mori*. *Mech. Dev.* 125: 411-420, 2008.
- Noda L. The Enzymes. Boyer PD (ed.), Academic Press, New York 8, pp 279-305, 1973.
- Ozyhar A, Kochman M. Juvenile-hormone-binding protein from the hemolymph of *Galleria mellonella* L. Isolation and characterization. *Eur. J. Biochem.* 162: 675-682, 1987.
- Qin L, Xia H, Shi H, Zhou Y, Chen L, Yao Q, *et al.* Comparative proteomic analysis reveals that caspase-1 and serine protease may be involved in silkworm resistance to *Bombyx mori* nuclear polyhedrosis virus. *J. Proteomics* 75: 3630-3638, 2012.
- Riddiford LM. Cellular and Molecular Actions of Juvenile Hormone I. General Considerations and Premetamorphic Actions, in: Evans PD (ed.), *In Advances in Insect Physiology*. Academic Press pp 213-274, 1994.
- Ritdachyeng E, Manaboon M, Tobe SS, Singtripop T. Molecular characterization and gene expression of juvenile hormone binding protein in the bamboo borer, *Omphisa fuscidentalis*. *J. Insect Physiol.* 58: 1493-1501, 2012.
- Sok AJ, Kamila C, Andrzej O, Marian K. The structure of the juvenile hormone binding protein gene from *Galleria mellonella*. *Biol. Chem.* 386: 2259-2210, 2005.
- Touhara K, Lerro KA, Bonning BC, Hammock BD, Prestwich GD. Ligand binding by a recombinant insect juvenile hormone binding protein. *Biochemistry* 32: 2068-2075, 1993.
- Truman JW, Riddiford LM. The origins of insect metamorphosis. *Nature* 401: 447-452, 1999.
- Vermunt AMW, Kamimura M, Hirai M, Kiuchi M, Shiotsuki T. The juvenile hormone binding protein of silkworm haemolymph: gene and functional analysis. *Insect Mol. Biol.* 10: 147-154, 2001.
- Wang GB, Zheng Q, Shen YW, Wu XF. Shotgun proteomic analysis of *Bombyx mori* brain: emphasis on regulation of behavior and development of the nervous system. *Insect Sci.* 23: 15-27, 2016.
- Wang MX, Lu Y, Cai ZZ, Liang S, Niu YS, Miao YG. Phenol oxidase is a necessary enzyme for the silkworm molting which is regulated by molting hormone. *Mol. Biol. Rep.* 40: 3549-3555, 2013.
- Xia Q, Guo Y, Zhang Z, Li D, Xuan Z, Li Z, *et al.* Complete resequencing of 40 genomes reveals domestication events and genes in silkworm *Bombyx*. *Science* 326: 433-436, 2009.
- Xia Q, Zhou Z, Lu C, Cheng D, Dai F, Li B, *et al.* A draft sequence for the genome of the domesticated silkworm *Bombyx mori*. *Science* 306: 1937-1940, 2004.
- Ye J, Fang L, Zheng H, Zhang Y, Chen J, Zhang Z, *et al.* WEGO: a web tool for plotting GO annotations. *Nucleic Acids Res.* 34: W293-297, 2006.
- Yi Q, Zhao P, Wang X, Zou Y, Zhong X, Wang C, *et al.* Shotgun proteomic analysis of the *Bombyx mori* anterior silk gland: An insight into the biosynthetic fiber spinning process. *Proteomics* 13: 2657-2663, 2013.
- Zhang P, Aso Y, Yamamoto K, Banno Y, Wang Y, Tsuchida K, *et al.* Proteome analysis of silk gland proteins from the silkworm, *Bombyx mori*. *Proteomics* 6: 2586-2599, 2006.

Supplementary material

Table S1 Primer sequences used for quantitative real-time PCR

Spot No. ^a	Protein name	Forward primer (5'-3')	Reverse primer (5'-3')
5	vacuolar ATP synthase subunit B	GCCTAGGCTCACTTACAAGACT	GACCAGAACGAAGGGTTCCA
12	juvenile hormone binding protein brP-2095 precursor	TGTTCAACACAAACGCCGAC	ACCCTTCGTAAACTCAGGCAG
14	adenylate kinase isoenzyme 1	CCCGGATCAGGAAAGGGAAC	CTCTCCGAGCCGCTTTTGAC
17	H ⁺ transporting ATP synthase subunit D	CTACTGCCGTATGACCAGAT	GACATAGTCGAGCTGCTCTT
	α-tubulin	CTCCCTCCTCCATACCCT	ATCAACTACCAGCCACCC

^a The spot number of identified proteins (see Table 1).

Table S2 The differentially expressed proteins and their identification through MALDI-TOF MS/MS

Material	Expression level ^b	Spot No.	Protein name	Accession No.	Mr(kDa)/pI ^c	Mascot scores	SC ^d (%)	Amino acid	Function	Fold change		
mq-m1 ^a	Up-regulated proteins	1	heat shock protein 70-3	AEI58998	72.82/5.12	138	25%	655	Molecular chaperone	1.7		
		4	uncharacterized protein LOC101738727	XP_012552185	49.91/5.29	129	31%	449	Unknown function	2.4		
		7	antitrypsin isoform 1	ACT36276	43.46/5.41	145	41%	392	Metabolism	1.8		
		10	alpha-tocopherol transfer protein-like	XP_004928929	35.28/5.56	146	47%	306	Transporter	2.9		
		11	alpha-tocopherol transfer protein-like	XP_004928929	35.28/5.56	183	50%	306	Transporter	2.5		
		13 ^e	cuticular protein RR-1 motif 34 precursor	NP_001166717	23.18/4.78	107	56%	207	Cell structure	3.9		
		15	tumor protein D54 isoform X3	XP_004930117	22.32/5.41	91	28%	206	Cell structure	1.9		
		16	putative cuticle protein	FAA00454	21.66/5.39	91	45%	215	Cell structure	2.2		
		20	odorant binding protein fmxg18C17 precursor	NP_001157372	26.48/6.23	121	28%	236	Cell structure	3.1		
		21	glutathione S-transferase sigma 1	NP_001037077	23.60/5.98	131	54%	206	Disease and defense	2.9		
		23	actin-depolymerizing factor 1	NP_001093278	17.23/6.17	175	64%	148	Cell structure	2.3		
			Down-regulated proteins	2	tubulin alpha-3 chain, partial	KFQ41598	43.57/5.79	197	55%	389	Cell structure	2.2
				3	beta-1 tubulin	TBB1_MANSE	50.65/4.75	262	64%	447	Cell structure	2.0
5	vacuolar ATP synthase subunit b			NP_001091828	54.67/5.25	187	55%	490	Metabolism	2.0		
6	antichymotrypsin-2			ACH2_BOMMO	41.43/5.26	109	39%	375	Metabolism	1.8		
9	annexin			BAB16697	36.11/4.89	138	43%	323	Disease and defense	2.0		
12	juvenile hormone binding protein brP-2095 precursor			NP_001036987	28.05/5.42	140	55%	249	Secondary metabolism	3.1		
14	adenylate kinase isoenzyme 1			XP_004929167	25.29/5.70	108	57%	226	Metabolism	1.9		
17	H ⁺ transporting ATP synthase subunit d			NP_001093279	20.19/5.56	57	52%	179	Metabolism	1.7		
19	triosephosphate isomerase			NP_001119730	26.93/5.67	168	64%	248	Metabolism	1.7		
22	cuticular protein RR-1 motif 42 precursor			NP_001166712	17.17/5.16	151	86%	159	Cell structure	3.0		

	Unique proteins	8	uncharacterized LOC101739385	XP_004922152	37.46/6.07	91	32%	328	Unknown function			
		18	transcription factor BTF3 homolog 4	XP_012551703	19.04/9.12	201	48%	174	Transcription			
		24	muscular protein 20	NP_001040476	20.29/8.70	79	20%	184	Cell structure			
mq-m2 ^a	Up-regulated proteins	1	heat shock protein 70-3	AEI58998	72.82/5.12	138	25%	655	Molecular chaperone	2.1		
		10	alpha-tocopherol transfer protein-like	XP_004928929	35.28/5.56	121	28%	306	Transporter	1.8		
		11	alpha-tocopherol transfer protein-like	XP_004928929	35.28/5.56	183	50%	306	Transporter	1.9		
		13	cuticular protein RR-1 motif 34 precursor	NP_001166717	23.18/4.78	107	56%	207	Cell structure	3.4		
		15	tumor protein D54 isoform X3	XP_004930117	22.32/5.41	91	28%	206	Cell structure	1.7		
		17	H ⁺ transporting ATP synthase subunit d	NP_001093279	20.19/5.56	57	52%	179	Metabolism	2.0		
		23	actin-depolymerizing factor 1	NP_001093278	17.23/6.17	175	64%	148	Cell structure	1.7		
		25	cuticular protein 66D	NP_729400	30.80/5.97	74	20%	270	Cell structure	2.5		
		26	cuticular protein RR-2 motif 67 precursor	NP_001166691	18.72/6.16	223	43%	178	Cell structure	8.6		
		28	ribosomal protein P2	NP_001037213	11.53/4.68	121	16%	112	Protein synthesis	2.4		
	Down-regulated proteins	5	vacuolar ATP synthase subunit b	NP_001091828	54.67/5.25	187	55%	490	Metabolism	2.3		
		6	antichymotrypsin-2 juvenile hormone binding protein	ACH2_BOMMO	41.43/5.26	109	39%	375	Metabolism	2.8		
		12	brP-2095 precursor	NP_001036987	28.05/5.42	140	55%	249	Secondary metabolism	11.1		
		14	adenylate kinase isoenzyme 1	XP_004929167	25.29/5.70	108	57%	226	Metabolism	2.1		
		18	transcription factor BTF3 homolog 4	XP_012551703	19.04/9.12	201	48%	174	Transcription	4.0		
		19	triosephosphate isomerase	NP_001119730	26.93/5.67	168	64%	248	Metabolism	1.6		
		20	odorant binding protein fmxg18C17 precursor	NP_001157372	26.48/6.23	121	28%	236	Cell structure	3.7		
		24	muscular protein 20	NP_001040476	20.29/8.70	79	20%	184	Cell structure	4.8		
	Unique proteins	22	cuticular protein RR-1 motif 42 precursor	NP_001166712	17.17/5.16	151	86%	159	Cell structure			
		27	uncharacterized protein LOC101741978	XP_004930780	16.55/4.93	117	46%	144	Unknown function			
mq-qc ^a	Up-regulated proteins	10	alpha-tocopherol transfer protein-like	XP_004928929	35.28/5.56	146	47%	306	Transporter	2.0		
		13	cuticular protein RR-1 motif 34 precursor	NP_001166717	23.18/4.78	107	56%	207	Cell structure	3.2		
		17	H ⁺ transporting ATP synthase subunit d	NP_001093279	20.19/5.56	57	52%	179	Metabolism	2.4		
		29	beta tubulin	NP_001036887	50.72/4.83	267	70%	447	Cell structure	1.9		
		30	centromere protein F isoform X2	XP_004926842	33.22/4.84	157	30%	297	Cell structure	1.7		
		32	cuticular protein RR-1 motif 3 precursor	NP_001166744	14.68/4.66	93	28%	137	Cell structure	2.4		
		33	cuticular protein RR-1 motif 3 precursor	NP_001166744	14.68/4.66	64	26%	137	Cell structure	2.5		
			Down-regulated proteins	5	vacuolar ATP synthase subunit b	NP_001091828	54.67/5.25	187	55%	490	Metabolism	1.8
				12	juvenile hormone binding protein brP-2095 precursor	NP_001036987	28.05/5.42	140	55%	249	Secondary metabolism	4.0
				14	adenylate kinase isoenzyme 1	XP_004929167	25.29/5.70	108	57%	226	Metabolism	1.7
		22	cuticular protein	NP_001166712	17.17/5.16	151	86%	159	Cell	4.4		

		RR-1 motif 42 precursor						structure	
	31	T-complex protein 1 subunit epsilon-like	XP_004933262	59.19/5.63	127	31%	542	Molecular chaperone	2.1
	34	thiol peroxidoredoxin	NP_001037083	22.07/6.09	252	18%	195	Disease and defense	2.5
	35	ubiquitin-like protein SMT3	NP_001037410	10.36/5.29	105	23%	91	Transcription	1.8
Unique proteins	7	antitrypsin isoform 1	ACT36276	43.46/5.41	145	41%	392	Metabolism	
	8	uncharacterized LOC101739385	XP_004922152	37.46/6.07	91	32%	328	Unknown function	
	26	cuticular protein RR-2 motif 67 precursor	NP_001166691	18.72/6.16	223	43%	178	Cell structure	
	27	uncharacterized protein LOC101741978	XP_004930780	16.55/4.93	117	46%	144	Unknown function	

^amq: silkworm from head capsule slippage (HCS) occurring; m1: silkworm from 12 h after HCS; m2: silkworm from 24 h after HCS; qc: newly molted fifth instar larvae; ^bReference gel: mq; ^cMW: Molecular weight; pl: Isoelectric point; ^dSC: Sequence coverage; ^eThe identified protein by MALDI-TOF MS.

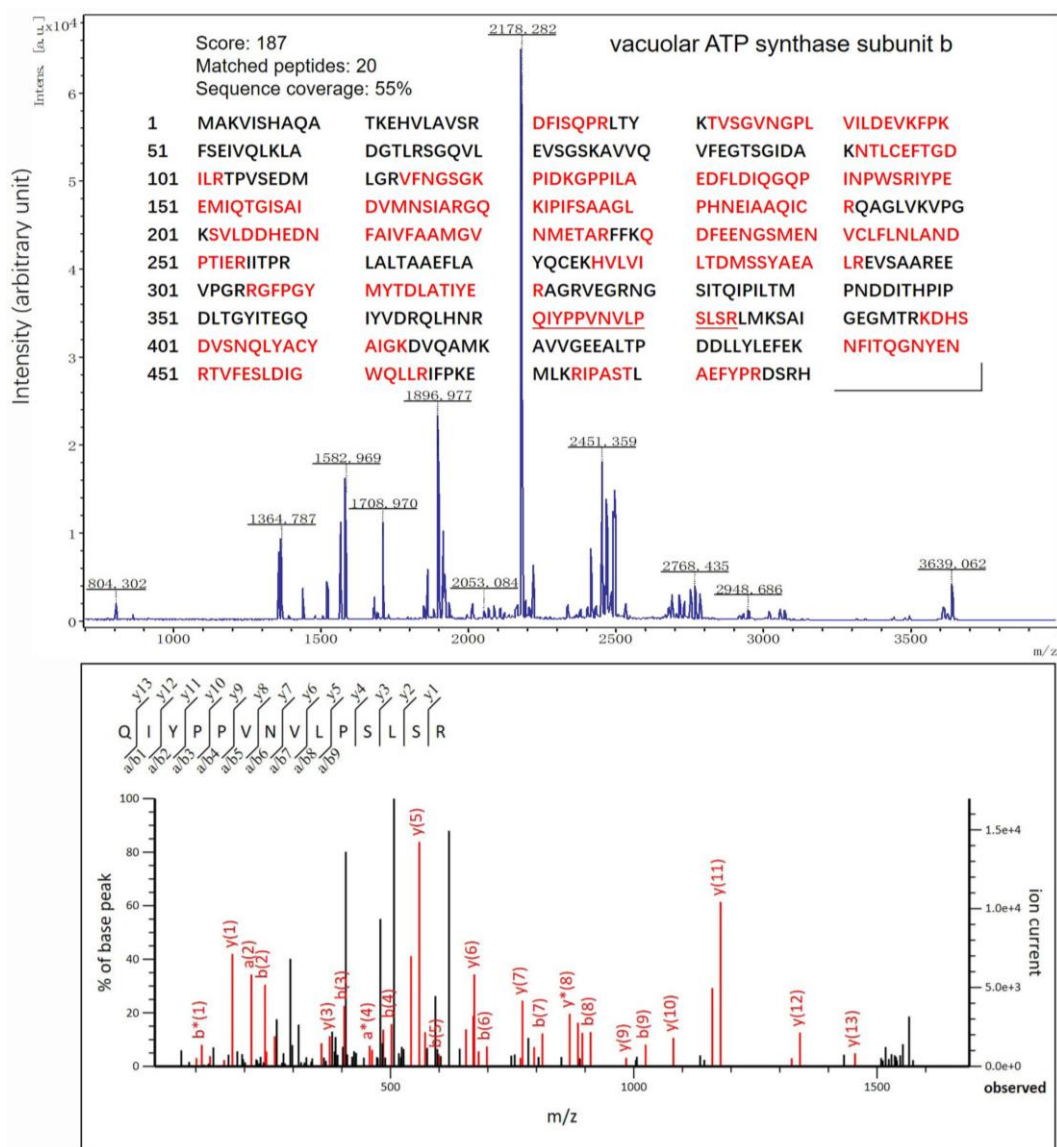


Fig. S1 The mass spectrogram of vacuolar ATP synthase subunit b and the amino acid assignment of the protein from the samples.

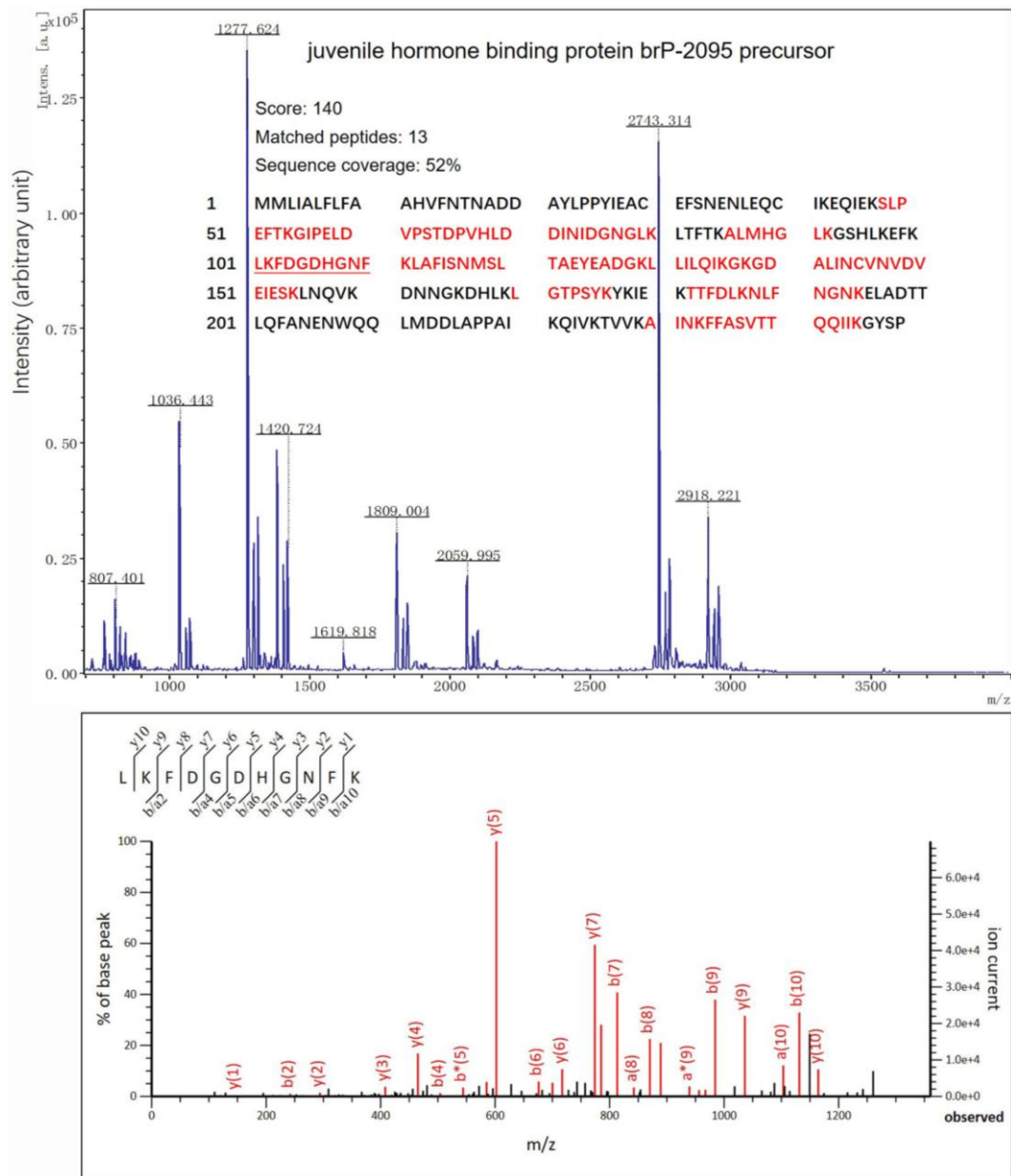


Fig. S2 The mass spectrogram of juvenile hormone binding protein brP-2095 precursor and the amino acid assignment of the protein from the samples.

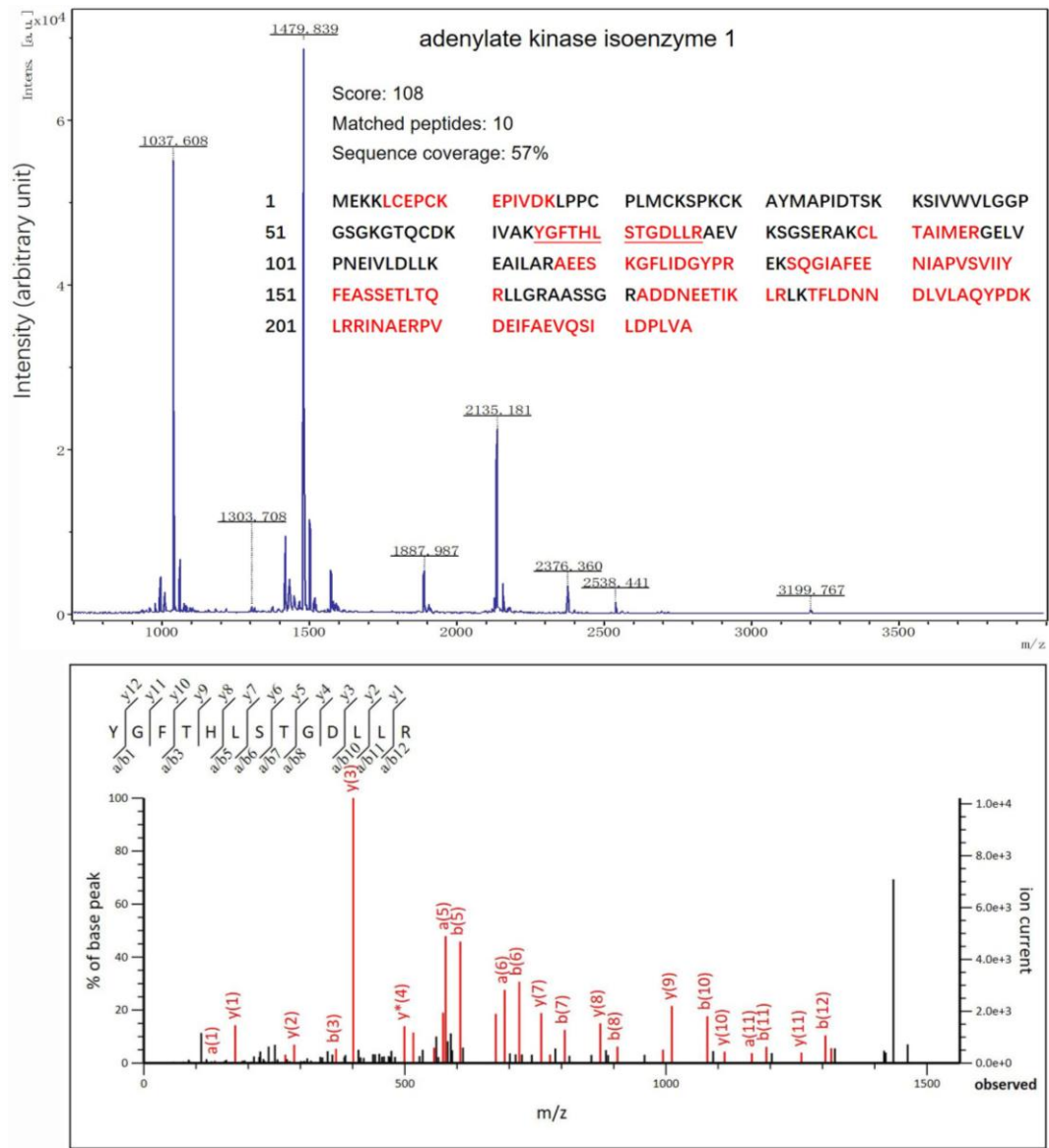


Fig. S3 The mass spectrogram of adenylylate kinase isoenzyme 1 and the amino acid assignment of the protein from the samples.